American Journal of Engineering and Applied Sciences

Original Research Paper

Development of Ionizing Radiation Sensors Based on Carbon Nanotubes

[1]Kenneth Fontánez, [1]Abraham García, [1]María del C Cotto-Maldonado, [1]José Duconge, [2]Carmen Morant, [2]Sergio Pinilla and [1]Francisco Márquez

[1]*Nanomaterials Research Group, School of Natural Sciences and Technology, Universidad Ana G. Méndez-Gurabo Campus, 00778PR, USA*
[2]*Department of Applied Physics, Universidad Autónoma de Madrid, 28049-Cantoblanco, Madrid, Spain*

Article history
Received: 05-04-2019
Revised: 13-05-2019
Accepted: 15-05-2019

Corresponding Author:
Francisco Márquez
Nanomaterials Research Group, School of Natural Sciences and Technology, Universidad Ana G. Méndez-Gurabo Campus, 00778PR, USA
Email: fmarquez@suagm.edu

Abstract: SWNTs have been efficiently grown on patterned substrates, for its subsequent application to the development of ionizing radiation sensors. SWNTs before and after exposure to X-rays were characterized by Raman and XPS spectroscopy, revealing the appearance of alterations that have been justified as possibly due to the presence of adsorbed oxygen species. These materials have been used for the fabrication of a sensor prototype that has shown a quasi-linear behavior as a function of the time of exposure to X-ray radiation.

Keywords: Sensor, Single-Walled Carbon Nanotubes, Ionizing Radiation, Resistivity

Introduction

Detection of ionizing radiation (Knoll, 1979) is relevant in different fields including energy, biological and nuclear research, national security and in applications such as monitoring the attrition of materials in space. Ionizing radiation detection systems are characterized by having a wide list of drawbacks, among which the following are included: Impossibility of reproducing stable signals (Knoll, 1979), manufacturing based on complicated and expensive stages (Owens, 2006), needs to work at low temperatures (Webster, 1999), low sensitivity (Graham *et al*., 1997) and even too voluminous sizes for proper use, as is the case of Geiger counters (Graham *et al*., 1997). Single-Walled carbon Nanotubes (SWNTs) are attracting much attention as promising materials for application in nanodevices due to their excellent electrical conductivity, optical, thermal and mechanical properties arising from their quasi-one-dimensional structure (Jorio *et al*., 2007). One of these potential applications is the use of SWNTs as radiation sensor. For this purpose, the critical steps in the design and fabrication of devices are focused on the growth of SWNTs into controlled architectures and onto appropriate substrates (Kong *et al*., 1998; Huang *et al*., 2002; Javey *et al*., 2005; He *et al*., 2005). Until now, the conventional way to obtain patterned Carbon Nanotubes (CNTs) is based in using a careful positioning of the metal catalyst (e.g., by evaporation, use of photoresist masks, or even Ar^+ sputtering) in localized positions, from where the CNTs grow (Hata *et al*., 2004; Zhong *et al*., 2007; Kawabata *et al*., 2008; Teo *et al*., 2001). Such catalyst patterning requires a precise control of the process with a long list of complicated steps. An easier method for depositing the catalyst consists in using a wet-based dip-coating approach, which provides some advantages in cost and scalability (Murakami *et al*., 2003). However, in this wet-based method the catalyst deposition at desired locations cannot use conventional lithographic techniques. A similar method (Xiang *et al*., 2010) has been used for patterning the growth of high-quality SWNTs on Si and SiO_2 based on the difference of surface wettability of the catalyst in both materials. In the literature, TiN has been chosen as a suitable electrically conductive supporting material for CNTs growth. This includes the use of TiN as the selected substrate (Rao *et al*., 2000; Campo *et al*., 2019) or as a barrier layer on crystalline Si (Pirio *et al*., 2002; De Los Arcos *et al*., 2004; Hiramatsu *et al*., 2005; García-Céspedes *et al*., 2009). When using a Si substrate, the formation of metal-silicides during the thermal treatment (annealing step) complicates the synthesis process. In fact, thin

layers of different compounds (TiO_2 (De Los Arcos *et al*., 2004), Ti (Srividya *et al*., 2010), TiN (De Los Arcos *et al*., 2004; Hiramatsu *et al*., 2005; García-Céspedes *et al*., 2009; Lin *et al*., 2009; Terrado *et al*., 2009), Al (De Los Arcos *et al*., 2004; Lin, *et al*., 2009) have been used to prevent the formation of metal-silicides. In this way, dense mats of vertically aligned multiwall carbon nanotubes have been grown on TiN substrates by using different precursors, including ferrocene (García-Céspedes *et al*., 2009) or different metals as Fe (De Los Arcos *et al*., 2004; Srividya *et al*., 2010; Lin *et al*., 2009), Ni (Terrado *et al*., 2009), Co (Hiramatsu *et al*., 2005) or Fe-Co (Le Normand *et al*., 2008) as catalysts. Besides its electrically conductive properties, TiN seems to increase the quality of the grown CNTs (i.e., much thinner CNTs with higher density as compared with those obtained on Si substrates) (Terrado *et al*., 2009; Campo *et al*., 2019). In the present research we have synthesized carbon nanotubes, using patterned substrates based on alternation of TiN and thermally grown SiO_2. In these substrates, the growth of carbon nanotubes has been produced specifically on TiN-free zones, generating a pattern of alternating lanes that has been the basis of the electrodes required for the use of these materials as radiation sensors. These materials have subsequently been exposed to X-ray irradiation, observing a clear correlation between the resistivity of the material and the radiation dose.

Experimental Section

Reagents

All chemicals used in this research were of analytical grade and were used as received without any further purification. Ethyl alcohol (99.9%) was provided by Sigma Aldrich. Si wafers (Si<100>, 300 µm thickness, p-type, single-side polished), were provided by El-CAT Inc. and used as substrates. Deionized water (Milli-Q, 18.2 MΩ.cm resistivity at 25°C) was used for all experiments.

Preparation of Substrates

Si (100) substrates, previously cleaned with isopropyl alcohol and dried in nitrogen flow, were oxidized by heat treatment at 200°C and vacuum (10^{-3} mbar). The thickness of SiO_2, estimated by SEM, was ca. 200 nm. Next, these substrates were coated with TiN by Physical Vapor Deposition (PVD). For this, a TiN target (99.99%) provided by Good fellows Cambridge Ltd., Huntingdon, England, was used. The deposition temperature was 100°C, with a deposition time of 90 min and a TiN tickness of ca. 100 nm. To define a specific pattern of alternating TiN and SiO_2 regions, the substrates were subsequently sputtered with a Kaufman-type ion-gun (Ion Tech Inc., 600 V and pressure of 10^{-4} mbar), by using a micrometric-sized patterned mask.

The preparation process to support the catalyst precursor has been described elsewhere (Morant *et al*., 2012). According to this procedure, the Co-Mo acetate solutions are deposited on the substrates by dip-coating with solutions of $Co(CH_3COO)_2{\cdot}4H_2O$ (0.02% v/v in ethanol) and $Mo(CH_3COO)_2$ (0.04% v/v in ethanol). From these solutions and after a calcination process in air at 400°C for 20 min, the catalysts are deposited on the surface of the substrates as metal oxides. These oxides will subsequently be reduced to metal, during the process prior to the growth of carbon nanotubes.

Characterization Techniques

The samples were characterized by Field Emission Scanning Electron Microscopy (FESEM), using a JEOL JM6400, operating at 20 kV. XPS measurements were performed on an ESCALAB 220i-XL spectrometer, by using the non-monochromated Mg Kα (1253.6 eV) radiation of a twin-anode, operating at 20 mA and 12 kV in the constant analyzer energy mode, with a PE of 50 eV. Raman spectra were acquired with a Renishaw spectrometer equipped with a 532-nm laser at 8 mW power and a nominal resolution of 5 cm^{-1}. The exposure of SWNTs samples to X-rays was carried out with an X-Pert PRO X-ray diffractometer, using the Cu-Kα X-radiation (λ = 1.5418 Å, 40 kV, 40 mA) at 45°. The resistivity measurements were carried out using a two-probe conductivity cell at 20°C and ambient conditions.

Growth of SWNTs

The synthesis of SWNTs was carried out by using a thermal Chemical Vapor Deposition (CVD) system, described elsewhere (Morant *et al*., 2012). In brief, this system is composed by a three-entry cylindrical quartz reactor with an inner diameter of 25 mm and a length of 1 m, installed inside a tubular furnace. The previously prepared substrates (TiN-SiO_2 grown on Si) were placed in a ceramic boat that was introduced within the quartz reactor. The system was then closed and evacuated to 5.10^{-3} mbar, using a membrane pump. After 10 min the pump was stopped and a mixture of N_2 (300 sccm) and H_2 (50 sccm) was incorporated into the reactor. Simultaneously, the reactor was heated up to 1123 K (5°C min^{-1}). Once the synthesis temperature was reached, the flow of N_2 was replaced by N_2 saturated with ethanol: water (99.5:0.5 v/v), keeping the flow of H_2 constant. The growth time was typically 5 min and the synthesis was completed by replacing the gas mixture with N_2 (250 sccm), until reaching room temperature (Fig. 1).

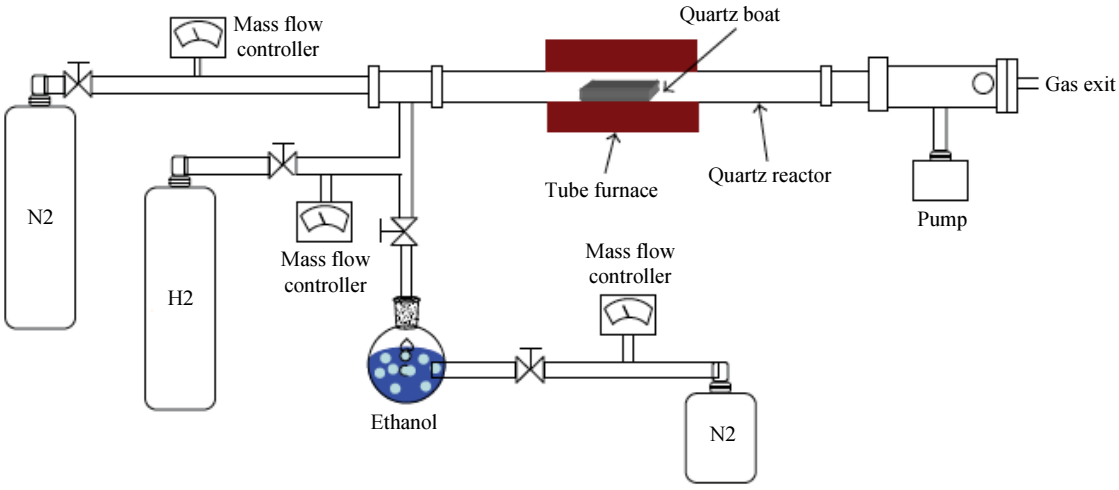

Fig. 1: Scheme of the CVD system used in this research

Results and Discussion

According to the procedure described above, the Co and Mo oxide nanoparticles are deposited specifically on the SiO_2 surfaces and not on the TiN lanes. This effect is due to the different Surface Free Energy (SFE) of SiO_2 and TiN and how it affects the materials that can be deposited efficiently on some surfaces and not on others. Once the substrates are introduced into the CVD system, together with the reactive gases and using a certain heating ramp, the oxides of Mo and Co are reduced to their metallic form, giving rise to the catalysts that will be efficient for the growth of SWNTs. These metallic nanoparticles will be located exclusively on the surface of SiO_2 and this is where the growth of SWNTs will take place (Fig. 2).

This behavior could be followed through XPS. After the deposition of the catalysts by dip-coating, the SiO_2 and TiN surfaces were analyzed. Figure 3 shows the photoelectron transitions corresponding to Co2p and Mo3d. As can be seen there, the intensities of Co and Mo are much greater when measured on the surface of SiO_2 than on that of TiN, indicating that most of the Co-Mo oxide nanoparticles are located on the surface of SiO_2. Co 2p has two main components at ca. 781.5 eV and 797.4 eV (Fig. 4a), assigned to the spin-orbit splitting of Co and specifically to a mixture of Co^{2+} and Co^{3+} due to the presence of Co_3O_4 (Lee *et al*., 2007). This result is also justified by the presence of satellite peaks (shoulders) at ca. 788 eV and 803 eV (Lee *et al*., 2007; Girardon *et al*., 2007). The results shown in the case of cobalt are similar to those observed for molybdenum and clearly indicate that metal oxide particles are deposited preferentially on the surface of SiO_2.

Figure 4 shows the SEM images of the SiO_2-TiN-Si substrates and how the metal oxide particles are deposited only on the surface of SiO_2 (Fig. 4a). When this substrate is used for the growth of SWNTs, it is precisely in the zones of SiO_2 where they grow (Fig. 4b).

SWNTs grown on SiO_2 according to the procedure described above were characterized by Raman spectroscopy, using a 532 nm laser source (Fig. 5). The Raman spectrum of the as-synthesized SWNTs (black line, Fig. 5) shows the G-band at 1587 cm^{-1} and the D-band at 1362 cm^{-1}. The high ratio of intensities of the G band to the D band (G/D ratio) reflects the high purity of the nanotubes, practically without defects or with very few defects (Dresselhaus *et al*., 2005). In addition, the signal of the Radial Breathing Modes (RBM) at frequencies below 300 cm^{-1} indicates that the nanotubes are SWNTs. The inset of Fig. 5 shows an expansion of the Raman spectrum in this region, whose Raman shift correlates with the diameter of the SWNT, by using the empirical formula $d = 248/\nu_B$ (Jorio *et al*., 2007), where ν_B is the corresponding Raman shift (cm^{-1}) and d is the diameter of the SWNT (nm). By using this expression, the average diameter of the synthesized nanotubes was estimated to be ca. 1.3 nm. To characterize the effect of the exposure of these SWNTs to ionizing radiation, this same sample was exposed to X-rays (average power of 1,600 W) for 40 min, using a fixed angle of 45°. Figure 5 (red line) shows the Raman spectrum of the SWNTs after the exposure of X-ray radiation. As can be seen there, the D-band experiences a slight increase in intensity, which is complemented by a decrease in intensity of the G-band. This effect can be correlated with an increase in the number of material defects due to radiation. Apparently and as it is deduced from the RBM band that does not undergo changes, this effect does not imply the modification of the average diameter of the material.

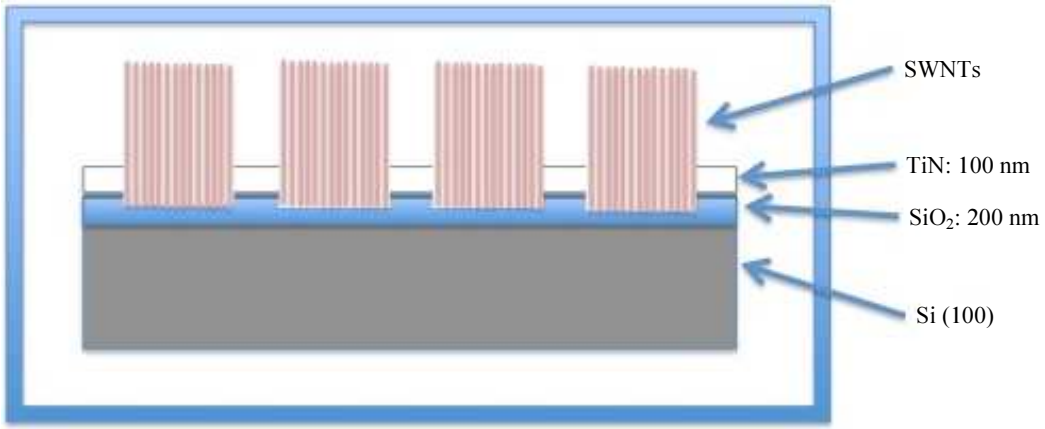

Fig. 2: Scheme of the selective growth of SWNTs on SiO_2 surfaces

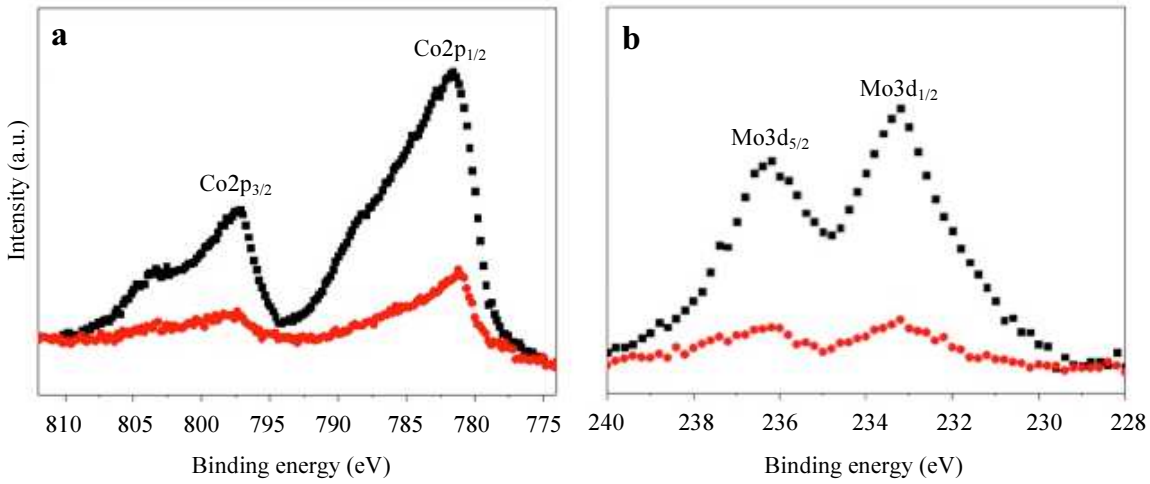

Fig. 3: XPS spectra of Co2p (a) and Mo3d (b) on SiO_2 (black) and TiN (red) surfaces, after catalyst deposition and subsequent calcinations at 673 K

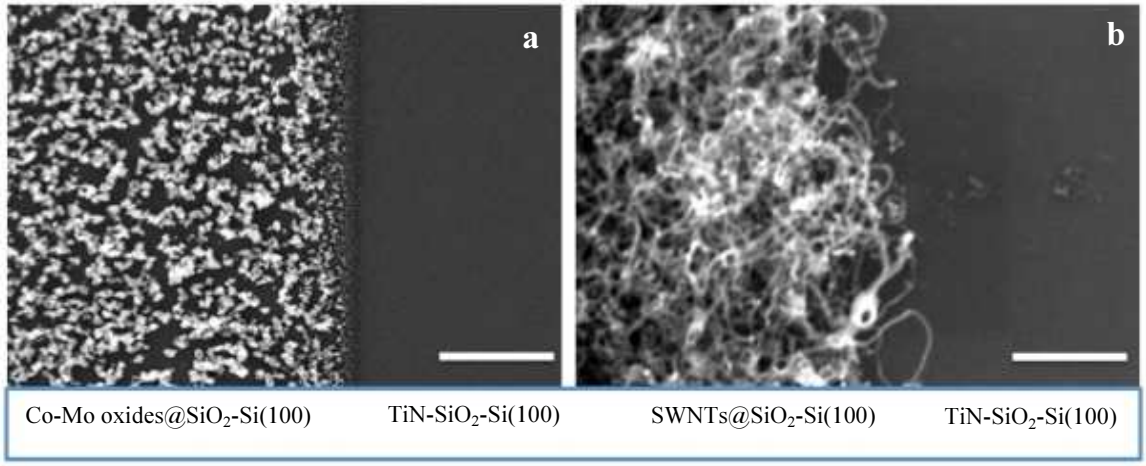

Fig. 4: SEM images of SiO_2-TiN patterned substrate, showing the selective deposition of metal oxide particles of Co and Mo over SiO_2 zones (a); and growth of SWNTs specifically on surfaces of SiO_2 and not on TiN (b). Bar = 50 nm

In order to analyze the origin of the changes observed by Raman spectroscopy, SWNT samples were analyzed before and after exposure to radiation by XPS. Figure 6a shows the C1s peak of the as-synthesized SWNTs (black line), showing a maximum at ca. 284.6 eV. This peak is symmetric and the binding energy, assigned to C-C bonds, is characteristic of SWNTs. When the sample is exposed to radiation (red line), the peak undergoes a widening, due possibly to the appearance of additional components at higher binding energy (arrow). Similar effects are observed when analyzing the O1s transition (Fig. 6b). The O1s peak of the non-irradiated sample shows a symmetric peak at ca. 531.5 eV that has been assigned to the presence of CO_2 and organic compounds with oxygen adsorbed on the surface of the SWNTs. When the sample is irradiated, this peak undergoes a widening, showing a shoulder at higher binding energy (indicated by an arrow). This shoulder could be due to the generation of radicals after irradiation, which could interact with the surface of SWNTs.

As already mentioned in the experimental section, SWNTs were grown in patterned substrates formed by alternating SiO_2 and TiN lanes. These substrates, with SWNTs grown on SiO_2, were adapted for the manufacture of radiation sensors, as shown in Fig. 7. For this, two Au collectors were incorporated, directly in contact on the Si substrate. Since the SWNTs are grown on SiO_2, which is a clearly insulating material, when measuring the resistivity between the two Au collectors, the only option for the circuit to close is that there was lateral electrical conduction between the nanotubes grown on the SiO_2. Thus, the prototype shown in Fig. 7 was exposed to different radiation doses, through the use of X-rays. After exposure to different times of irradiation, the resistivity of the material was measured using a two-probe conductivity cell at ambient conditions and room temperature. Figure 8 shows the observed variation in resistivity as the sensor is subjected to increasing times of exposure to X-rays. As can be seen, there is a quasi-linear relationship between the exposure time and the increase in resistivity, which could allow the use of these systems in the development of efficient ionizing radiation sensors.

There are many unknowns about the effects that are occurring on SWNTs due to radiation. How does the presence of organic compounds affect the surface of the nanotubes and therefore the potential appearance of radicals or other species that can modulate the conduction properties of these materials, is one of the issues that are currently being analyzed. On the other hand, if the electrical conduction properties of SWNTs depend on the presence of possible adsorbed compounds on the surface of these materials and how these can be transformed by the applied radiation effect, we could consider that these detection systems are not irreversible, being able to be "rebooted" simply by means of a thermal treatment that allows to eliminate these compounds from the surface to be used again. In this regard, different studies are currently being developed to better understand what processes are occurring and how these materials can be efficiently used in the development of ionizing radiation sensors.

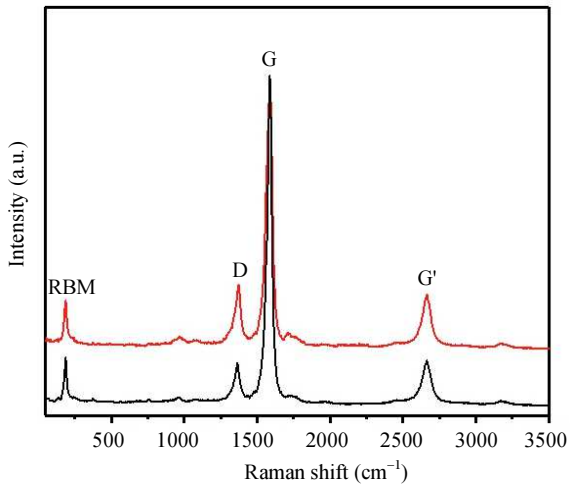

Fig. 5: Raman spectrum of the as-synthesized SWNTs (black line) and after exposure to X-ray radiation (1,600 W) for 40 min (red line)

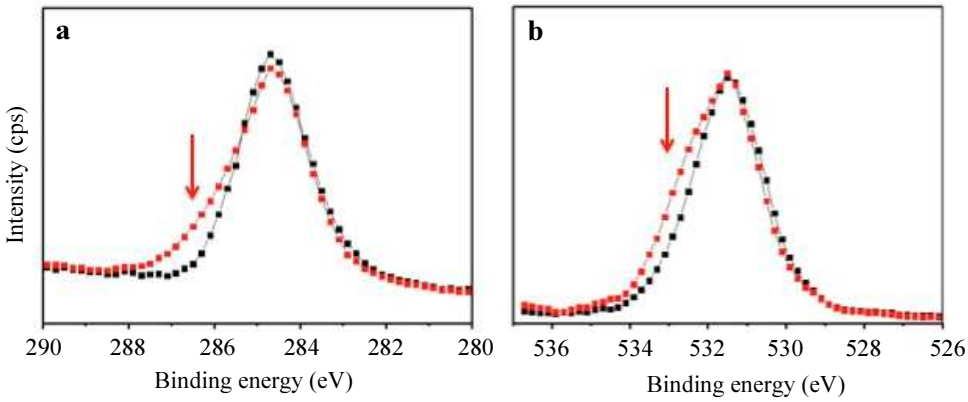

Fig. 6: C1s (a) and O1s (b) XPS peaks of the as-synthesized SWNTs (black line) and after exposure to irradiation (red line)

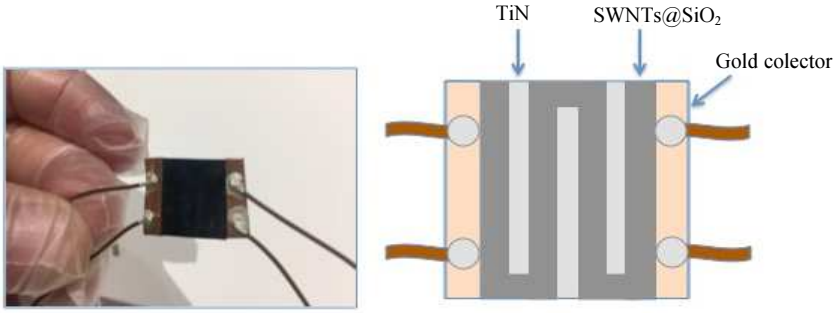

Fig. 7: Image of the manufactured prototype (left) and scheme of the device (right)

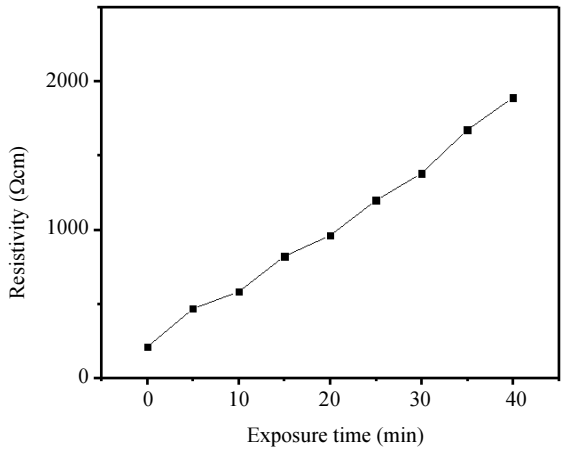

Fig. 8: Variation of the average resistivity as a function of the time of exposure to X-rays

Conclusion

SWNTs have been efficiently grown on patterned substrates. According to Raman spectroscopy, these SWNTs showed very few defects and were used for the fabrication of a prototype ionizing radiation sensor, based on the modulation of the resistivity as a function of the time of exposure to radiation. The modulation of the resistivity has been interpreted as due to the presence of oxygenated compounds adsorbed on the surface of SWNTs. These compounds are possibly altered during the X-ray radiation, generating changes in the properties of the SWNTs that ultimately result in the increase in the resistivity of the material as the time of exposure to X-rays increases.

Future work will be required to accurately identify the processes responsible for the observed changes and how these materials can be applied to the commercial development of radiation sensors.

Acknowledgement

KF thanks The Puerto Rico Louis Stokes Alliance for Minority Participation (PR-LSAMP) for a research sholarship. AG thanks the Consortium for Integrating Energy System in Engineering and Science Education, CIESESE (DENA0003330), for a postgraduate scholarship.

Funding Information

Financial support from the U.S. Department of Energy, through the Massie Chair Project at Universidad del Turabo, from the U.S. Department of Defense under Grant W911NF-14-1-0046, from MINECO under Grant ENE2014-57977-C2-1-R and from the US Department of Energy and the Consortium for Integrating Energy System in Engineering and Science Education, CIESESE (DENA0003330), is gratefully acknowledged.

Author's Contributions

All authors contributed equally to this work.

Ethics

This article is original and contains unpublished material. The corresponding author confirms that all of the other authors have read and approved the manuscript and no ethical issues involved.

References

Campo, T., S. Pinilla, S. Gálvez, J.M. Sanz and F. Márquez *et al*., 2019. Synthesis procedure of highly densely packed carbon nanotube forests on TiN. Nanomater.

De Los Arcos, T., M.G. Garnier, P. Oelhafen, D. Mathys and J.W. Seo *et al*., 2004. Influence of the buffer layer on the growth rate and characteristics of the carbon nanotubes grown by CVD. Carbon, 42: 187-190. DOI: 10.1016/j.carbon.2003.10.020

Dresselhaus, M.S., G. Dresselhaus, R. Saito, A. Jorio, 2005. Raman spectroscopy of carbon nanotubes. Physics Reports, 409: 47–99. DOI: 10.1016/j.physrep.2004.10.006

García-Céspedes, J., S. Thomasson, K.B.K. Teo, I.A. Kinloch and W.I. Milne *et al*., 2009. Efficient diffusion barrier layers for the catalytic growth of carbon nanotubes on copper substrates. Carbon, 47: 613-621. DOI: 10.1016/j.carbon.2008.10.045

Girardon, J.S., E. Quinet, A.G. Constant, P.A. Chernavskii, L. Gengembre, A.Y. Khodakove, 2007. Cobalt dispersion, reducibility, and surface sites in promoted silica-supported Fischer-Tropsch catalysts. J. Catal., 248: 143-157. DOI: 10.1016/j.jcat.2007.03.002

Graham, S.C., R.H. Friend, S. Fung and S.C. Moratti, 1997. The effect of X-ray irradiation on poly(*p*-phenylene vinylene) and derivatives. Synth. Met., 84: 903-904. DOI: 10.1016/S0379-6779(96)04204-X

Hata, K., D.N. Futaba, K. Mizuno, T. Namai and M. Yumura *et al*., 2004. Water-assisted highly efficient synthesis of impurity-free single-walled carbon nanotubes. Science, 306: 1362-1364. DOI: 10.1126/science1104962

He, M.S., X. Ling, J. Zhang and Z.F. Liu, 2005. Surfactant-resisted assembly of Fe-containing nanoparticles for site-specific growth of SWNTs on si surface. J. Phys. Chem. B, 109: 10946-10951. DOI: 10.1021/jp051127j

Hiramatsu, M., H. Nagao, M. Taniguchi, H. Amano and Y. Ando *et al*., 2005. High-rate growth of films of dense, aligned double-walled carbon nanotubes using microwave plasma enhanced chemical vapor deposition. Jpn. J. Appl. Phys., 44: L693-L695. DOI: 10.1143/JJAP.44.L693

Huang, S.M., L.M. Dai and A.W.H. Mau, 2002. Controlled fabrication of large-scale aligned carbon nanofiber/nanotube patterns by photolithography. Adv. Mater., 14: 1140-1143. DOI: 10.1002/1521-4095(20020816)14:16<1140::AID-ADMA1140>3.0.CO;2-5

Javey, A. and H.J. Dai, 2005. Regular arrays of 2 nm metal nanoparticles for deterministic synthesis of nanomaterials. J. Am. Chem. Soc., 127: 11942-11943. DOI: 10.1021/ja0536668

Jorio, A., M.S. Dresselhaus and G. Dresselhaus, 2007. Carbon Nanotubes: Advanced Topics in the Synthesis, Structure, Properties and Applications. 1st Edn., Springer, Berlin, ISBN-10: 3540728651, pp: 720.

Kawabata, A., S. Sato, H. Shioya, T. Iwai and M. Nihei *et al*., 2008. Direction-controlled growth of carbon nanotubes. Jpn. J. Appl. Phys., 47: 1975-1977. DOI: 10.1143/JJAP.47.1975

Knoll, G.F., 1979. Radiation Detection and Measurement. 1st Edn., John Wiley and Sons Inc., New York, ISBN-10: 047149545X, pp: 816.

Kong, J., H.T. Soh, A.M. Cassell, C.F. Quate and H.J. Dai, 1998. Synthesis of individual single-walled carbon nanotubes on patterned silicon wafers. Nature, 395: 878-881. DOI: 10.1038/27632

Le Normand, F., C.T. Fleaca, M. Gulas, A. Senger and O. Ersen *et al*., 2008. Growth of vertically oriented films of carbon nanotubes by activated catalytic chemical vapor deposition on Fe-Co/TiN/Si(100) substrates. J. Mater. Res., 23: 619-631. DOI: 10.1557/JMR.2008.0097

Lee, J.M., J.W. Kim, J.S. Lim, T.J. Kim, S. D. Kim, S.J. Park, Y.S. Lee, 2007. X-ray Photoelectron Spectroscopy Study of Cobalt Supported Multi-walled Carbon Nanotubes Prepared by Different Precursors. Carbon Science, 8: 120-126. DOI: 10.5714/CL.2007.8.2.120

Lin, N., H. Wang, P. Dixit, T. Xu and S. Zhang *et al*., 2009. Investigation of carbon nanotube growth on multimetal layers for advanced interconnect applications in microelectronic devices nanostructured materials, carbon nanotubes and fullerenes. J. Electrochem. Soc., 156: K23-K27. DOI: 10.1149/1.3060347

Morant, C., T. Campo, F. Márquez, C. Domingo and J.M. Sanz *et al*., 2012. Mo–Co catalyst nanoparticles: Comparative study between TiN and Si surfaces for single-walled carbon nanotube growth. Thin Solid Films, 520: 5232-5238. DOI: 10.1016/j.tsf.2012.03.099

Murakami, Y., Y. Miyauchi, S. Chiashi and S. Maruyama, 2003. Direct synthesis of high-quality single-walled carbon nanotubes on silicon and quartz substrates. Chem. Phys. Lett., 377: 49-54. DOI: 10.1016/S0009-2614(03)01094-7

Owens, A., 2006. Semiconductor materials and radiation detection. J. Synchrotron Rad., 13: 143-150. DOI: 10.1107/S0909049505033339

Pirio, G., P. Legagneux, D. Pribat, K.B.K. Teo and M. Chhowalla *et al*., 2002. Fabrication and electrical characteristics of carbon nanotube field emission microcathodes with an integrated gate electrode. Nanotechnology, 13: 1-4. DOI: 10.1088/0957-4484/13/1/301

Rao, A.M., D. Jacques, R.C. Haddon, W. Zhu and C. Bower *et al*., 2000. In situ-grown carbon nanotube array with excellent field emission characteristics. Applied Phys. Lett., 76: 3813-3815. DOI: 10.1063/1.126790

Srividya, S., S. Gautam, P. Jha, P. Kumar and A. Kumar *et al*., 2010. Titanium buffer layer for improved field emission of CNT based cold cathode. Applied Surf. Sci., 256: 3563-3566. DOI: 10.1016/j.apsusc.2009.12.155

Teo, K.B.K., M. Chhowalla, G.A.J. Amaratunga, W.I. Milne and D.G. Hasko *et al*., 2001. Uniform patterned growth of carbon nanotubes without surface carbon. Applied Phys. Lett., 79: 1534-1536. DOI: 10.1063/1.1400085

Terrado, E., I. Tacchini, A.M. Benito, W.K. Maser and M.T. Martinez, 2009. Optimizing catalyst nanoparticle distribution to produce densely-packed carbon nanotube growth. Carbon, 47: 1989-2001. DOI: 10.1016/j.carbon.2009.03.045

Webster, J.G., 1999. The Measurement, Instrumentation and Sensors: Handbook. 1st Edn., CRC Press, ISBN-10: 3540648305, pp: 2506.

Xiang, R., E. Einarsson, H. Okabe, S. Chiashi and J. Shiomi *et al*., 2010. Patterned growth of high-quality single-walled carbon nanotubes from dip-coated catalyst. Jpn. J. Applied Phys., 49: 02BA03-1-02BA03-3. DOI: 10.1143/JJAP.49.02BA03

Zhong, G.F., T. Iwasaki, J. Robertson and H. Kawarada, 2007. Growth kinetics of 0.5 cm vertically aligned single-walled carbon nanotubes. J. Phys. Chem. B, 111: 1907-1910. DOI: 10.1021/jp067776s